Thermopower and electrical conductivity of $Ca_{3-x}Y_xMn_2Ge_3O_{12}$ garnet

G. Oversluizen,* T.H.J.M. Kuijpers, and R. Metselaar
Laboratory of Physical Chemistry, Eindhoven University of Technology, P.O. Box 513, 5600-MB Eindhoven, The Netherlands
(Received 27 September 1983)

The conductivity and thermopower of several electronically conducting, polycrystalline $Ca_{3-x}Y_xMn_2Ge_3O_{12}$ samples in the composition range $0 \leq x \leq 2$ have been measured in the temperature range 30—1000 °C. The conductivities are thermally activated while the thermopower is temperature independent. These results are shown to be consistent with adiabatic hopping of small polarons localized on the manganese sublattice. The number of available transport sites is reduced by defect interactions. The mobilities are thermally activated with $E_a \sim 0.62$ eV for $0 \leq x \leq 1.75$ and $E_a = 0.79$ eV for $x = 2$. The calculated optical-phonon frequencies agree well with the recorded infrared lattice spectra.

I. INTRODUCTION

The garnets form a large group of compounds that crystallize in the cubic system with space group O_h^{10} ($Ia3d$). The general formula is $\{C_3\}[A_2](D_3)O_{12}$ where $\{C\}$ denotes ions on dodecahedral sites, $[A]$ denotes ions on octahedral sites, and (D) denotes ions on tetrahedral sites. The different sublattices can accommodate a variety of cations: C for rare-earth ions Y, Ca, and Na; A for Al, Mg, Mn, and Fe; and D for Al, Si, Ge, V, and Fe. The crystallographic unit cell contains 8 formula units.

Because of their technological importance, ferrimagnetic iron garnets have been widely studied.[1] In the iron garnets many of the observed interesting physical properties, including light-induced changes of the magnetic permeability, are due to small amounts of Fe^{2+} ions present on the Fe^{3+} sublattices.[2] The localized nature of the excess electrons is of utmost importance for the occurrence of photoinduced effects. However, the presence of transition-metal ions in several sublattices constitutes an extra complication in the understanding of the charge-transport mechanism and photoconductivity results.[3,4] For this reason we have started a study of garnets in which transition-metal ions are only found in one sublattice. In recent papers the electrical and optical properties of $\{Ca_2Na\}[Mg_2](V_3)O_{12}$ were discussed. In this compound a number of V^{4+} centers, analogous to the Fe^{2+} centers in the iron garnets, were introduced by reduction.[5–7]

In this paper, results of conductivity and thermopower measurements on $\{Ca_{3-x}Y_x\}[Mn_x^{2+}Mn_{2-x}^{3+}](Ge_3)O_{12}$ are presented. The end members with $x = 0$ and 2 were already known to exist.[8,9] Because Y^{3+} is very stable, charge compensation occurs on the manganese sublattice and the Mn^{2+} concentration can be chemically controlled from 0—100 at. % (sublattice occupation) by yttrium substitution. In this way we obtain a series of compounds which enables us to study the behavior of charge carriers over a wide range of concentrations. In Sec. II the relevant theory is recalled. In Sec. III the preparation of the garnet powders is described together with the characterization by means of x-ray and electron-microprobe analysis, and Sec. IV gives experimental details. In Sec. V the results are presented and discussed in relation to the literature and the conclusions drawn are summarized in Sec. VI.

II. THEORY

A. Polaronic conduction

The garnets studied here belong to the transition-metal oxides. In these oxides the small overlap between the d orbitals of adjacent cations may result in a narrow rigid-ion bandwidth and concomitant small electron velocities. Electron-phonon coupling leads to the formation of polarons. We consider only the case where the lattice distortion created by the charge carrier is confined to distances of the order of the lattice constant the so-called small polaron.[10] Depending on the value of the electron transfer integral (J), with respect to the phonon energy $h\nu_0$, two cases are considered. If $J > h\nu_0$, the so-called adiabatic case, an electron can tunnel several times between the potential wells during an excited lattice state. At high temperatures $T > \frac{1}{2}\Theta$ ($h\nu_0 = k\Theta$) an approximate formula for the mobility reads

$$\mu = (1-c)\frac{ea^2}{kT}\nu_0 \exp\left[-\frac{E_h}{kT}\right], \tag{1}$$

where c is the fraction of occupied sites, a is the intersite distance, E_h is the hopping energy, and the other symbols have their usual meaning. If $J \ll h\nu_0$, the nonadiabatic case, the mobility is of the form

$$\mu = (1-c)\frac{ea^2}{\hbar}\frac{J^2}{E_h^{1/2}(kT)^{3/2}} \exp\left[-\frac{E_h}{kT}\right]. \tag{2}$$

In both cases the mobility is thermally activated. In the high-temperature region in which we are interested here, the extra $T^{-1/2}$ in Eq. (2) with respect to Eq. (1) is hardly of interest.

Apart from electron-phonon coupling, localization of charge carriers may also be brought about by electron-

electron correlation and/or disturbances of the periodic potential such as dopants, disorder, dislocations, etc.[11] The localization of electrons due to the correlation energy has recently been considered by Thouless.[12] Basically the localization comes about because the energy gain achieved by band formation, which is proportional to the width of the band, is insufficient to overcome the electrostatic repulsion between the electrons. This mechanism has been suggested for several transition-metal mono-oxides and for magnetite where the inter-transition-metal ion distance is smaller than in the garnets discussed here (i.e., larger rigid-ion bandwidths[13–15]).

With respect to the effect of disturbances of the periodic potential, theoretical model calculations were performed by Anderson.[16] If the disorder is sufficiently large, localized states in the band gap are formed, and Anderson estimated that above a critical value of the ratio of the disorder potential (U) and the rigid-ion bandwidth (Δ) $U/\Delta > 2.8$, all states are localized. Of course, one should expect that electrons which are already localized due to disorder interact with phonons and form small polarons, and vice versa, small polarons will tend to be localized at sites of low potential energy. Austin and Mott[17] applied the theory (developed by Miller and Abrahams[18] for heavily doped broad-band semiconductors) to polar materials, and argue that at the high temperatures used in this study, the conductivity (σ) behaves as $\sigma \sim B/T[\exp(-E_a/kT)]$ with $E_a = E_h + \frac{1}{2}E_d$, where E_d is the spread in energy levels caused by disorder and E_h is the hopping energy [cf. Eq. (1)].

In the yttrium-doped manganese garnets the electron localization probably emanates from the combined action of electron-phonon coupling, electron-correlation terms, and electron-dopant interactions. Thus the electron mobility is thermally activated, and a part of the observed activation energy (E_a) is due to site-energy differences caused by defect interactions. These differences result in the creation of preferred conduction pathways and thereby reduce the number of available transport sites. It will be shown (Sec. V) that the results to be discussed in this paper can be consistently interpreted using Eq. (1).

B. Thermoelectric power in electronically conducting solids

Since the treatment of Onsager it has been firmly established that the Seebeck coefficient, defined as the open-circuit voltage (ΔV) developed across a material in a temperature gradient divided by the temperature difference (ΔT) in the limit $\Delta T \to 0$, can be expressed as[19]

$$\alpha \equiv -\Delta V/\Delta T = -S^*/e \equiv -(1/e)(\bar{S} + Q^*/T) , \quad (3)$$

where S^* (equal to J_s/J_e), the ratio between the entropy flux (J_s) and the particle flux (J_e), is called the transported entropy, $\bar{S}$ is the particle entropy, and Q^* is the heat transferred by the particle.

If electrical transport occurs via thermally activated hopping of a fixed number of localized charge carriers, then the entropy term is largely determined by the entropy of mixing; $S_{\text{mix}} = k \ln[(1-c)/c]$, where c is the fraction of occupied transport sites. There is considerable evidence, from both practical and theoretical studies, that the heat of transfer is negligible.[10,17,20] The resultant thermopower is temperature independent,

$$\alpha = -(k/e)\ln[(1-c)/c] . \quad (4)$$

According to this relation, $\alpha < 0$ for $0 \le c \le \frac{1}{2}$, and $\alpha > 0$ for $\frac{1}{2} \ge c \ge 1$, where c is defined as $c = n/N$, and n and N are the concentrations of carriers and available sites, respectively. With $N = N_0$, the total concentration of transition-metal ions concerned, Eq. (4) is known as the "Heikes" formula.[21] It is important to note that in both n- and p-type material, electrical transport occurs by hopping of the same electrons over the same lattice sites. Consequently, interaction effects are to be expected at the high concentrations used in this study. This is in contrast to band-type conduction where electron and hole transport take place at different energy levels in independent bands, and their contributions to the thermopower can be added weighted by the transport numbers (t): $\alpha_{\text{total}} = t_e\alpha_e + t_h\alpha_h$.

III. PREPARATION AND CHARACTERIZATION

$Ca_{3-x}Y_xMn_2Ge_3O_{12}$ powders have been prepared by solid-state reaction. The component oxides and carbonates, Y_2O_3, GeO_2 and $CaCO_3$, $MnCO_3$, were of at least p.a. purity grade. Weighed stoichiometric quantities were repeatedly fired at temperatures in the range 1000–1150 °C for a total of 90–140 h. The mixing of the starting materials and the remixing between the firings was performed by conventional ball-milling in agate mortars. Following the original synthesis of $Ca_3Mn_2Ge_3O_{12}$ and $CaY_2Mn_2Ge_3O_{12}$ by Mill[8] and Geller *et al.*,[9] the materials with $x = 0$ and $x \neq 0$ were fired in air and nitrogen, respectively. After the first firing, samples with $x \neq 0$ usually contained $Y_2Ge_2O_7$. Finally, after refiring, all diffraction lines present in the recorded x-ray patterns could be indexed in the $Ia3d$ space group exclusively. The obtained powders were pelletized using steel molds at pressures $\sim 2 \times 10^8$ Pa and sintered in air ($x = 0$) or nitrogen ($x \neq 0$) at temperatures in the range 1100–1200 °C for ~ 60 h. Densities varied from 58 to 88% of the theoretical density.

The x-ray-diffraction lines were slightly broadened in some cases, probably indicating inhomogeneities in the yttrium distribution. This could not be verified with the electron microprobe, however. Though the x-ray patterns did not show spurious lines, a few spots of a second phase were detected by electron microscopy in the samples with $x = 1.75$ and 2. This second phase only contained Y and Ge in equal amounts and is therefore probably the remainder of the $Y_2Ge_2O_7$ phase which occurs at the beginning of the solid-state reaction. Because of the localized character and the small concentration this second phase is not expected to have a marked influence on the conductivity and thermopower data presented in Sec. V.

IV. EXPERIMENTAL DETAILS

The cylindrically shaped samples, typically 5–10 mm thick and 8 mm in diameter, were spring-mounted between platinum electrodes in an Al_2O_3 sample holder. Good electrical contact was achieved by platinum painting

of the contact areas (Leitplatin 308A Demetron). Most of the conductivity measurements were performed with a Keithley 616 Digital Electrometer operating in the resistance mode. At high temperatures four-point measurements were also made using a Knick JS 300 Precision-Current/Voltage Source as a current source and the Pt wires of the measurement thermocouples served as voltage probes connected to the Keithley 616. The results of the two-point and four-point measurements were in excellent agreement with each other. The systems were occasionally checked for frequency dispersion in the range $0.05-10^4$ Hz with a Solartron Frequency Response Analyzer (model no. 1174). The sample holder was furnished with two platinum-wire resistance-heating elements, capable of being independently controlled, to supply the temperature gradient for the thermopower measurements. With the use of two heating blocks the average temperature is easily maintained constant within $\pm 1\,^{\circ}\mathrm{C}$, while the ΔT range is effectively doubled without increasing $\Delta T_{\max}$ because the temperatures can be inverted. The thermal response of the system is such that a few minutes after a change of settings the thermocouple readings have stabilized within 1 μV. To assure good correspondence, thermopower and conductivity measurements were performed directly after one another. The Seebeck coefficients were calculated by a least-squares analysis from plots of ΔV vs ΔT consisting of eight data points and the maximum temperature difference employed was limited to $\sim 10\,^{\circ}\mathrm{C}$. These plots were linear and with an uncertainty of $\pm 1\,^{\circ}\mathrm{C}$ they always went through the origin (apart from exceptions at high temperatures which are explicitly discussed in the following section). At low temperatures the measurement range is limited by the sample resistance. At resistance values higher than $\sim 5\times 10^6\ \Omega$, electrical noise caused by the heating coils and spurious voltages, both inevitably present, lead to erratic results. The reported Seebeck coefficients are not affected by the heating currents, since operating the system at the same average temperature, 30° and 150°, respectively, above the temperature of the main furnace, resulted in identical thermopower values.

Infrared lattice spectra were recorded in the (100—1000)-cm^{-1} region using a Bruker infrared Fourier-transform spectrometer. For the (100—700)-cm^{-1} region the finely divided powder samples were embedded in polyethylene, and for the (400—1000)-cm^{-1} region the samples were embedded in KBr pressed pellets.

V. RESULTS AND DISCUSSION

Measurements on polycrystalline specimens are always hampered by possible grain-boundary effects. Therefore the resistance was checked for Ohmic behavior and occasionally the frequency dispersion characteristics were recorded. This should also reveal an ionic contribution to the conductivity. Thus it was ascertained that the measured data correspond to electronic bulk conductivities (σ). In Fig. 1 the results for a number of $Ca_{3-x}Y_xMn_2Ge_3O_{12}$ samples with $0\le x\le 2$ are plotted as $\log(\sigma T)$ versus reciprocal temperature. Only data points for $x=0$ and 2 have been drawn to avoid confusion. The σ values have been corrected for porosity using $\sigma=\sigma_m(1-V)^{-3/2}$ where σ_m is the measured conductivity and V is the volume fraction of the pores.[22] Inspection of the figures shows that the conductivities can be fitted to a relation of the form

$$\sigma=\frac{Nc(1-c)e^2a_{\nu_0}^2}{kT}\exp\left[-\frac{E_a}{kT}\right], \tag{5}$$

i.e., assuming adiabatic hopping of small polarons where N is the total density of transport sites and the other symbols have been assigned before. The activation energies and pre-exponential factors calculated by least-squares analyses are summarized in Table I.

The above interpretation is supported by the thermopower data shown in Fig. 2. These data represent values corrected for the thermopower of the platinum measurement leads.[23] All samples exhibit a practically temperature-independent thermopower apart from some high-temperature data which will be discussed separately below. This strongly suggests a constant number of carriers. In Fig. 3 the Seebeck coefficients measured at 500 K are plotted versus $\log_{10}[c/(1-c)]$, where it has been assumed that the Mn^{2+} concentration corresponds to the yttrium content ($c=x/2$). Evidently the points do not fit the Heikes formula [Eq. (4)]. In recent literature it has

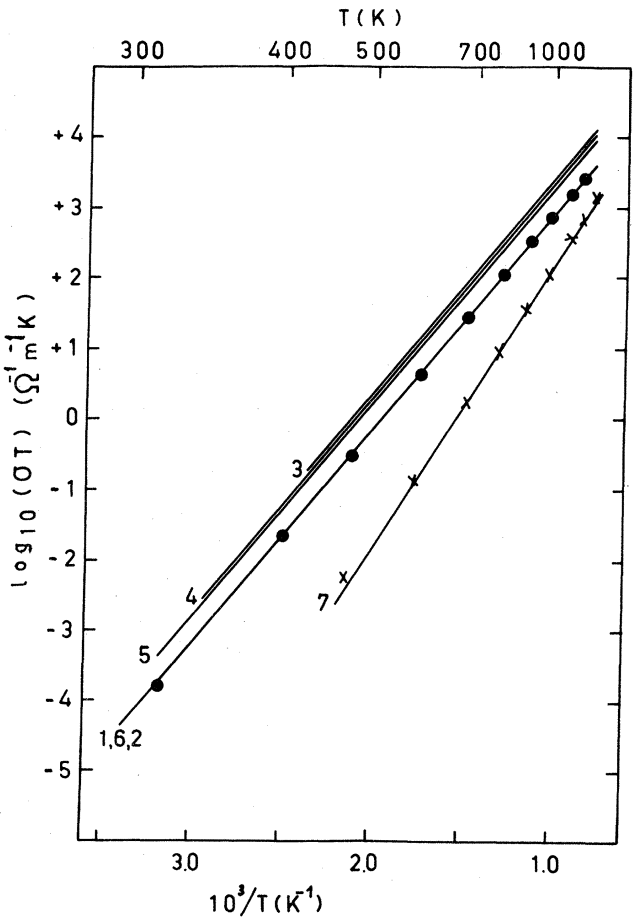

FIG. 1. Conductivity-temperature product vs reciprocal temperature for $Ca_{3-x}Y_xMn_2Ge_3O_{12}$ samples with (1) $x=0$, (2) $x=0.1$, (3) $x=0.67$, (4) $x=1$, (5) $x=1.5$, (6) $x=1.75$, and (7) $x=2$.

TABLE I. Parameters obtained by fitting conductivity data for $Ca_{3-x}Y_xMn_2Ge_3O_{12}$ samples to Eq. (5); μ is the mobility.

Composition x	E_a (eV)	$Nc(1-c)e^2a^2\nu_0/k$ ($10^6\ \Omega^{-1}m^{-1}K$)	$\mu_{500\,K}$ ($10^{-11}\ m^2V^{-1}s^{-1}$)
0	0.61	1.19	
0.1	0.63	1.67	1.5
0.67	0.63	4.43	0.53
1	0.62	3.40	0.29
1.5	0.61	2.75	0.18
1.75	0.63	1.51	0.080
2	0.79	1.78	0.0014

been argued that this formula should be adapted to include spin degeneracy of the carriers.[24–26] If the system is to remain electron-hole symmetric this results in $198\log_{10}[c/2(1-c)]$ for small values of x (n type) and $198\log_{10}[2c/(1-c)]$ for large values of x (p type); to our knowledge no theory has been proposed yet for the intermediate concentration region. The dashed lines in Fig. 3 correspond to these equations. In the n-type region the difference between experiment and theory is enlarged whereas in the p-type region reasonable agreement is attained. However, in our opinion, the dashed lines should be disregarded. The reason is that for a transition-metal ion with a net spin in both valence states, the spin degeneracy should not contribute to the mixing entropy. A similar argument has been used for the case of Fe_3O_4 by Hodge and Bowen.[27]

To reconcile the data with Eq. (4), we therefore propose that the number of possible transport sites is reduced due to defect interactions. This means that of the two Mn ions per formula unit only a number $z=x/c$ is available for polaron transport. The effective number of transport sites (z) can be calculated from the known yttrium content (x) and the fraction of occupied transport sites (c), evaluated from the thermopower data using Eq. (4). The results are shown in Table II. Assuming equal activation energies and negligible variations in ν_0 upon incorporation of yttrium ions the conductivities should scale with the

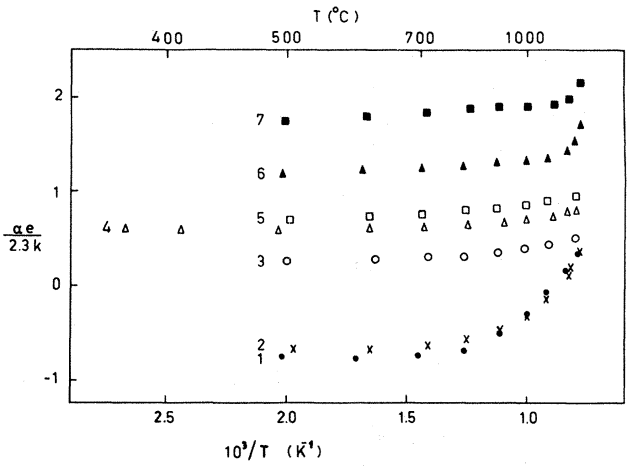

FIG. 2. Reduced Seebeck coefficient vs reciprocal temperature for $Ca_{3-x}Y_xMn_2Ge_3O_{12}$ samples with (1) $x=0$, (2) $x=0.1$, (3) $x=0.67$, (4) $x=1$, (5) $x=1.5$, (6) $x=1.75$, and (7) $x=2$.

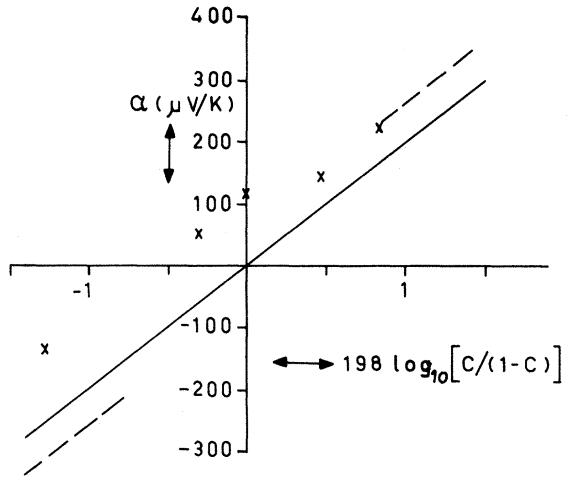

FIG. 3. Comparison of experimental Seebeck coefficients at $T=500$ K with theoretical values: Solid line denotes "Heikes" formula; dashed lines denote Heikes formula including an electron-spin degeneracy factor (see text).

product $z(1-c)c$. In view of the restrictions discussed below the scaling apparent from Fig. 4 is satisfactory. The deviation observed for the sample with $x=1.5$ may be related to the fact that this sample was fired much longer than the other compositions. Annealing of samples during a week at 1100 °C in air indeed resulted in changes of thermopower and conductivity.

However, a very remarkable result is observed when the z values from Table II are plotted against x (Fig. 5). The figure shows that the number of Mn sites available for the polarons increases nearly linearly with x; z approaches the theoretical maximum $z=2$ for $x\to 2$. Thus for $CaY_2Mn_2Ge_3O_{12}$ the number of available sites is equal to the total number of Mn ions. From the value of the preexponential term in Eq. (5), as given in Table I, we can calculate the frequency ν_0. The lattice constants of the end members are $a_0=1.232$ nm for $x=0$ and 1.247 nm for $x=2$, in accordance with literature data.[8,9] For the intermediate compounds we found an approximately linear variation of a_0 with x, as measured from Guinier pictures. This corresponds to a density of Mn ions $N_0=8.3\times10^{27}$ m^{-3} and a nearest-neighbor Mn-Mn distance $a=\frac{1}{4}a_0\sqrt{3}=0.54$ nm. The resulting frequency is $\nu_0=2.3\times10^{13}\ s^{-1}$. Figure 6 gives the infrared spectrum

TABLE II. Thermopower and effective fraction of transport sites in $Ca_{3-x}Y_xMn_2Ge_3O_{12}$ as a function of the yttrium content.

Composition x	α (μV/K)	c	$z=x/c$	$zc(1-c)$
0	−149	0.151		
0.1	−135	0.173	0.578	0.083
0.67	54	0.651	1.03	0.234
1.0	113	0.788	1.27	0.212
1.5	139	0.834	1.80	0.248
1.75	232	0.937	1.87	0.110
2.0	347	0.983		

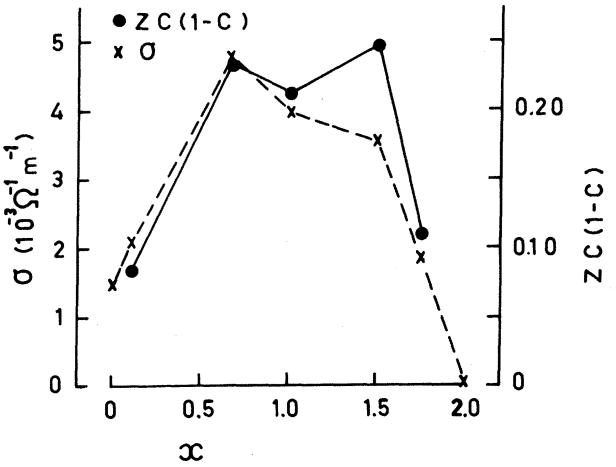

FIG. 4. Comparison of composition dependencies at 500 K of electrical conductivity and the $zc(1-c)$ product (see text) for $Ca_{3-x}Y_xMn_2Ge_3O_{12}$ (lines are drawn to guide the eye).

of a manganese garnet with $x=0.1$. The spectrum shows the features typical for all garnets, viz., a set of bands in the (800—600)-cm^{-1} region and a strong band in the region around 400 cm^{-1}. Similar spectra are known for rare-earth aluminum, gallium, and iron garnets.[28] For $Y_3Al_5O_{12}$ the optical phonons have been studied by measurements of ir reflection spectra and the Raman effect.[29] By comparison it is seen that the LO modes in the manganese garnet cover the region 200—900 cm^{-1}, i.e., $(0.6–2.7)\times10^{13}$ s^{-1}. These values agree well with the ν_0 calculated above.

The correct magnitude of ν_0 sustains the applicability of the adiabatic small-polaron model since for the nonadiabatic case the apparent frequency $\nu=J^2\hbar\sqrt{EkT}$ [cf. Eqs. (1) and (2)] would be much smaller because then $J\ll h\nu_0$. From Eq. (1) we can derive the polaron mobility μ. Table I shows μ values calculated at $T=500$ K. The low values observed, are consistent with the small polaron model. The number of other garnet materials where the charge-

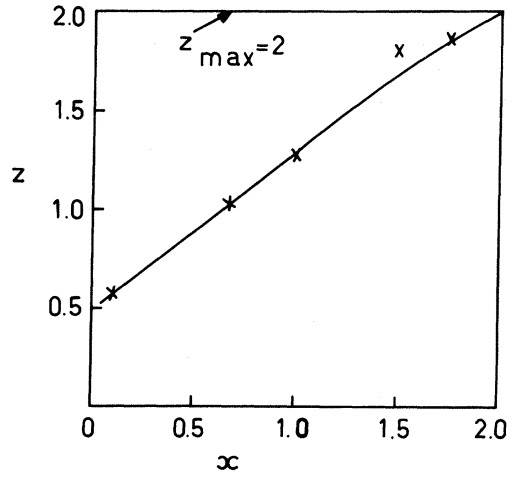

FIG. 5. Number of available Mn transport sites per formula unit of $Ca_{3-x}Y_xMn_2Ge_3O_{12}$ as a function of x.

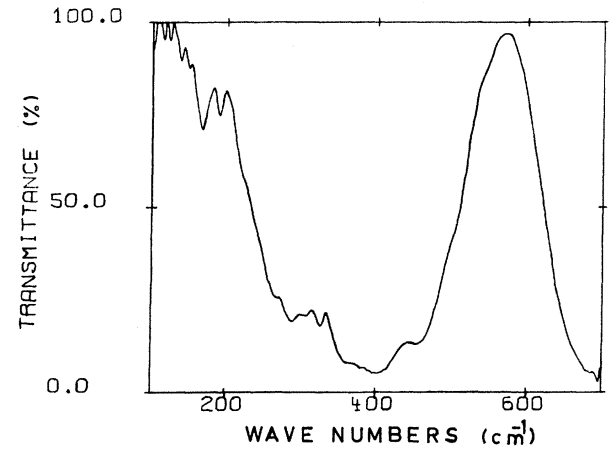

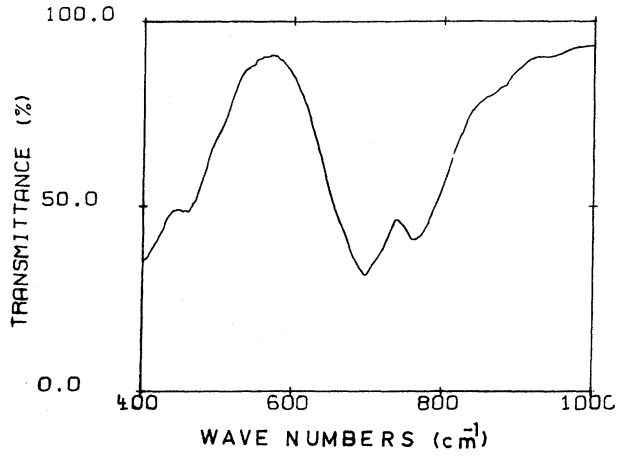

FIG. 6. Infrared-absorption spectra of $Ca_{2.9}Y_{0.1}Mn_2Ge_3O_{12}$ at room temperature for the (100—700)-cm^{-1} and (400—1000)-cm^{-1} regions.

transport mechanism has been established is limited and mainly concerns doped and undoped yttrium iron garnet. For this compound the majority of the experimental results favor the applicability of the large-polaron model in the high-temperature region $T>600$ K.[4] On the other hand, in gadolinium and dysprosium iron garnet the charge transport has been ascribed to thermally activated hopping of holes via the iron lattice sites with mobilities $\mu_{500\,K}\sim10^{-10}$ m^2/V sec.[30,31]

Finally, the deviations of the thermopower data at high temperatures will be discussed. The data for this temperature region are questionable because a corresponding change in conductivity was not observed. Further, annealing of the specimens for several hours in nitrogen did not affect the measured conductivity and thermopower values, so a change in defect concentration due to reduction can be ruled out. It was observed, however, that with increasing temperature the linear thermovoltage ΔV-vs-ΔT plots tended to be displaced away from the origin, indicating additional voltages. Since at high temperatures the ionic defects will become increasingly mobile, these additional voltages, that lead to erratic thermopower values, are

probably caused by compositional relaxation in the temperature gradient.

VI. CONCLUSIONS

The electrical transport in $Ca_{3-x}Y_xMn_2Ge_3O_{12}$, with $0 \leq x \leq 2$, occurs via adiabatic hopping of small polarons localized on the manganese sublattice, where defect interactions limit the number of available transport sites. In electronically conducting oxides with a fixed number of carriers localized on a transition-metal sublattice the spin degeneracy does not contribute to the mixing entropy if the cation has a net spin in both valence states involved.

ACKNOWLEDGMENTS

The authors wish to thank H. J. M. Heijligers for performing the electron-microprobe analyses and J. A. van Beek and D. L. Vogel for recording the infrared lattice spectra.

---

*Present address: Philips Research Laboratories, P.O. Box 80000, 5600-JA, Eindhoven, The Netherlands.

[1]G. Winkler, *Magnetic Garnets* (Vieweg, Braunschweig, 1981).
[2]R. Metselaar, *Interaction of Radiation with Condensed Matter* (IAEA, Vienna, 1977), Vol. 2, p. 159.
[3]R. Suryanarayanan and R. Krishnan, Phys. Status Solidi A 22, K177 (1974).
[4]R. Metselaar and P. K. Larsen, in *Physics of Magnetic Garnets,* edited by A. Paoletti (North-Holland, New York, 1978), p. 417.
[5]G. Oversluizen and R. Metselaar, J. Phys. C 15, 4869 (1982).
[6]G. Oversluizen and R. Metselaar J. Phys. C 16, 355 (1983).
[7]G. Oversluizen and R. Metselaar, in *Solid State Chemistry 1982,* edited by R. Metselaar, H. J. M. Heijligers, and J. Schoonman (Elsevier, Amsterdam, 1983), p. 353.
[8]B. V. Mill, Zh. Strukt. Khim. 6, 471 (1965).
[9]S. Geller, C. E. Miller, and R. G. Treuting, Acta Crystallogr. 13, 179 (1960).
[10]A. J. Bosman and H. J. van Daal, Adv. Phys. 19, 1 (1970).
[11]D. Adler, in *Handbook on Semiconductors,* edited by W. Paul (North-Holland, Amsterdam, 1982), Vol. I, Chap. 13, p. 805.
[12]D. J. Thouless, J. Phys. (Paris) Colloq. 37, C4-349 (1976).
[13]B. H. Brandow, Adv. Phys. 26, 651 (1977).
[14]N. F. Mott, in *Festkörperprobleme XIX,* edited by J. Treusch (Vieweg, Braunschweig, 1979), p. 331.
[15]M. I. Klinger and A. A. Samokhvalov, Phys. Status Solidi B 79, 9 (1977).
[16]P. W. Anderson, Phys. Rev. 109, 1492 (1958).
[17]I. G. Austin and N. F. Mott, Adv. Phys. 18, 41 (1969).
[18]A. Miller and E. Abrahams, Phys. Rev. 120, 745 (1960).
[19]R. R. Heikes and R. W. Ure, in *Thermoelectricity,* edited by R. R. Heikes and R. W. Ure (Interscience, New York, 1961), Chap. 2.
[20]H. L. Tuller and A. S. Nowick, J. Phys. Chem. Solids 38, 859 (1977).
[21]R. R. Heikes, in *Thermoelectricity,* Ref. 19, Chap. 4.
[22]D. A. G. Bruggeman, Ann. Physik 25, 645 (1936).
[23]J. P. Moore and R. S. Graves, J. Appl. Phys. 44, 1174 (1973).
[24]P. M. Chaikin and G. Beni, Phys. Rev. B 13, 647 (1976).
[25]D. P. Karim and A. T. Aldred, Phys. Rev. B 20, 2255 (1979).
[26]C. C. Wu, S. Kumarakrishnan, and T. O. Mason, J. Solid State Chem. 37, 144 (1981).
[27]J. D. Hodge and H. K. Bowen, J. Am. Ceram. Soc. 64, 431 (1981).
[28]N. T. McDevitt, J. Opt. Soc. Am. 59, 1240 (1969).
[29]J. P. Hurrell, S. P. S. Porto, I. F. Chang, S. S. Mitra, and R. P. Bauman, Phys. Rev. 173, 851 (1968).
[30]V. R. Yadav and H. B. Lal, Can. J. Phys. 57, 1204 (1979).
[31]V. R. Yadav and H. B. Lal, Jpn. J. Appl. Phys. 18, 2229 (1979).